

SINR Distribution and Scheduling Gain Analysis of Uplink Channel-Adaptive Scheduling

Shotaro Kamiya¹, Student Member, IEEE, Koji Yamamoto², Member, IEEE,
Seong-Lyun Kim³, Member, IEEE, Takayuki Nishio⁴, Member, IEEE,
and Masahiro Morikura⁵, Member, IEEE

Abstract—Despite the widespread popularity of stochastic geometry analysis for cellular networks, most analytical results lack the perspective of channel-adaptive user scheduling. This study presents a stochastic geometry analysis of the SINR distribution and scheduling gain of normalized SNR-based scheduling in an uplink Poisson cellular network, in which the per-user truncated fractional transmit power control is performed. Because the effects of multi-user diversity depend on the number of candidate users to be scheduled, which is a random variable in a Poisson cellular network, the number distribution of candidate users is a major factor in analyzing the SINR distribution of user scheduling. However, the maximum transmit power constraint of users complicates the distribution of candidate users. This study provides the number distribution of candidate users in a general form, which is obtained by modeling the area of the existing range of candidate users using a beta distribution. Based on this result, this study successfully obtains the uplink SINR distribution under channel-adaptive user scheduling, including cases in which edge users are both allowed and not allowed to transmit at the maximum transmit power. Numerical evaluations reveal that the scheduling gain varies depending on the SNR and the fraction of edge users.

Index Terms—Stochastic geometry, uplink cellular networks, user scheduling, power control, scheduling gain.

I. INTRODUCTION

THE methodology through which the performance analysis of a wireless network is conducted has changed dramatically during the past decade because of the emergence of stochastic geometry [1]–[3]. This type of performance analysis is conventionally conducted using Monte Carlo simulations, which are often time-consuming, as when, for example, an appropriate system parameter setting is sought. By contrast,

Manuscript received September 26, 2018; revised March 10, 2019, July 26, 2019, and November 26, 2019; accepted December 19, 2019. Date of publication January 10, 2020; date of current version April 9, 2020. This work was supported in part by the JSPS KAKENHI Grant JP17J04854 and in part by the KDDI Foundation. The associate editor coordinating the review of this article and approving it for publication was J. Yuan. (Corresponding author: Shotaro Kamiya.)

Shotaro Kamiya, Koji Yamamoto, Takayuki Nishio, and Masahiro Morikura are with the Graduate School of Informatics, Kyoto University, Kyoto 606-8501, Japan (e-mail: kamiya@imc.cce.i.kyoto-u.ac.jp; kyamamot@i.kyoto-u.ac.jp).

Seong-Lyun Kim is with the School of Electrical and Electronic Engineering, Yonsei University, Seoul 120-749, South Korea (e-mail: slkim@yonsei.ac.kr).

Color versions of one or more of the figures in this article are available online at <http://ieeexplore.ieee.org>.

Digital Object Identifier 10.1109/TWC.2019.2963866

stochastic geometry provides a direct and often tractable mathematical expression of performance metrics (e.g., signal-to-interference-plus-noise power ratio (SINR) distribution and average rate) for different types of wireless networks [1]. More specifically, the modeling of random topologies based on a point process, typically a Poisson point process (PPP), results in a simple and tractable form of SINR distribution.

Stochastic geometry analysis has been extensively applied to downlink cellular networks [3], [4]. Andrews *et al.* [5] proposed a basic framework for a downlink cellular analysis and derived the SINR distribution $\mathbb{P}(\text{SINR} > \theta)$ as a simple result, which is in good agreement with Monte Carlo simulations. In addition, owing to the recent emergence of symmetric traffic applications (e.g., video streaming and cloud-based tasks [6]), analysis of uplink cellular networks has become more important. Therefore, the framework of downlink analysis has been extended to an uplink case [7], [8], and their extensions have appeared in a wide variety of scenarios [9]–[12].

A. Related Works: Commonalities and Differences

An uplink analysis fundamentally differs from a downlink analysis in that the locations of the transmitters are correlated and that per-user power control is performed [8]. Novlan *et al.* [7] derived the uplink coverage probability for a randomly chosen user (i.e., a typical user) under fractional power control by ignoring the correlation among active user locations, which simplifies the calculation but maintains the accuracy of the derived results. ElSawy and Hossain [8] presented a tractable framework for an uplink cellular network, in which they considered the channel inversion power control of users and ignored edge users, who do not have sufficient power to compensate completely for the exponential decay path loss owing to the maximum power constraint. These assumptions enabled the authors of [8] to drop the marginalization with respect to the contact distance and to derive tractable results. However, we would like to emphasize that a channel-adaptive user scheduling was not considered in any of the aforementioned studies. In other words, the results includes only cases in which the transmitting user is selected uniformly randomly in each cell. In modern cellular systems, the transmitting user is not selected uniformly randomly but

rather based on a specific channel-adaptive scheduling [13] such as the proportional fair scheduler [14].

The authors of [15], [16] derived the complementary cumulative distribution function (ccdf) of the SINR and the average data rate of a channel-adaptive user scheduling in a downlink cellular network. They assumed that the transmission of users in each cell follows the normalized signal-to-noise power ratio (SNR)-based scheduling [17], in which the scheduler in the cell selects the user having the largest instantaneous SNR normalized by the short-term average SNR. The authors ensured that a stochastic geometry analysis was possible by considering the largest order statistic [18] when modeling the fading gain of the scheduled user. The analysis captures the topological randomness in a cellular network, which was not considered in other conventional analyses of channel-adaptive scheduling [17], [19]–[22].

In this study, we derived the SINR ccdf and the average data rate of a typical scheduled user under the normalized SNR-based scheduling in an uplink Poisson cellular network with truncated fractional power control. As previously discussed, an uplink analysis essentially differs from a typical downlink analysis [5] in that per-user power control is performed. We thus consider truncated fractional power control as per-user power control. Simultaneously, we consider the policy regarding edge users in two ways: according to whether they are allowed to transmit at the maximum transmit power, as in [7], [23], or not allowed to transmit, as in [8]. Therefore, this study considers a more general transmit power control that includes those presented in [7] or [8]. In addition, we consider the reduction of interference owing to the cells that include no transmitting user, whereas in a typical uplink analysis [7], [8] the locations of users are arranged such that each BS has at least one scheduled user.

This study was presented in part at IEEE ICC 2018 [24]. In [24], we presented the SINR distribution of normalized SNR-based scheduling in an uplink Poisson cellular network. This study extends the contents of [24] in the following ways.

- This study employs truncated fractional power control instead of the truncated channel inverse power control [8], which was employed in [24]. As previously mentioned, the truncated fractional power control is a generalization of truncated channel inverse power control. Therefore, this study provides an SINR distribution in a more general form. In addition, this study considers not only cases in which edge users are not allowed to transmit but also those in which edge users are allowed to transmit at the maximum transmit power. By contrast, [24] includes only the first case.
- This study derives the number distribution of candidate users in a more general form than that in [24], which includes only the asymptotically exact distributions.
- This study considers not only the case where only one user is supported in a single resource block but also that where multiple users are supported in a single resource block (Section IV-A), whereas [24] considers only the first case.

- This study considers not only a perfect channel state information (CSI) assumption but an imperfect CSI assumption (Section IV-B), whereas [24] considers only the first assumption.

B. Contributions

A noteworthy difference between uplink and downlink scheduling analyses is the number distribution of candidate users, which is the users that can potentially be assigned a resource block in each cell. In the analysis of user scheduling, the number of candidate users is a critical factor because the multi-user diversity gain increases along with the number of candidate users. Note that the number of candidate users is a random variable because of the inherent randomness of the positions of base stations (BSs) and users in Poisson cellular networks. As discussed later in detail, the probability mass function (pmf) of the number of candidate users in an uplink network varies depending on the fraction of edge users, whereas the pmf in a downlink network is unique [15] given the BS and user densities. Therefore, to derive the SINR distribution in a general form, we must develop a pmf of the number of candidate users for uplink networks that is applicable regardless of the fraction of edge users. In Section III-B.1, this study first provides two pmfs for two special cases: those in which all users in an entire cell are candidate users and those in which the users near the cell edges are not candidate users. The two pmfs are shown to be asymptotically equal to the exact number distributions of the candidate users. Then, in Section III-B.2 we provide the general pmf using beta distribution fitting, which requires a relatively high calculation cost and is yet applicable regardless of the fraction of edge users.

The contributions of this study are as follows.

- For an uplink Poisson cellular network, we derive the conditional SINR distribution of a typical scheduled user given the number of candidate users. The conditional SINR distribution is a component of the complete SINR distribution, which is averaged over the pmf of the number of candidate users. In addition, this study considers two ways of handling edge users, that is, according to whether they are allowed to transmit at the maximum transmit power or are not allowed to transmit at all. We also show that the conditional SINR distribution is simplified by assuming a perfect channel inversion power control and by not allowing edge users to transmit. Furthermore, we show that the analytical expression is reduced to a closed-form expression for certain special cases.
- We provide the pmf of the number of candidate users in each cell in an uplink network, by which we then derive the marginalized SINR distribution under uplink user scheduling. This study clarifies that the pmf of the number of candidate users depends on the BS density and achievable range, which is the maximum contact distance induced by the maximum power constraint, for a case in which edge users are not allowed to transmit.

We derive the pmf of the number of candidate users in a general form using beta distribution fitting, including the asymptotic case in which the BS density is sufficiently large or small. Note that the number of candidate users is a critical factor, not only for multi-user diversity but also for other analyses that depend on the number of users, such as the probability that a randomly chosen user is assigned a resource block [25].

- The numerical evaluations of the derived analytical results confirm that normalized SNR-based scheduling increases the coverage probability because of multi-user diversity gain. We show that the improvement in the SINR varies depending on the ratio of edge users and the SNR of a scheduled user. To investigate the degree of multi-user diversity, we also evaluate the scheduling gain, which is defined as the ratio of the average rate of a specific scheduling to that of round-robin scheduling, and is thus the performance metric of the specific scheduling. The evaluation shows that the scheduling gain decreases as the ratio of edge users increases.

If we do not consider a user scheduling (i.e., each BS selects a user regardless of instantaneous fading gain), the resulting performance metric is underestimated compared to the actual value. The generalized analyses given in this study will be useful for estimating the degree of multi-user diversity according to a given situation, and will help in effectively operating a user scheduler. In addition, the analytical results will help in providing insight into the design of cell deployment when considering the scheduling gain based on the number of accommodated users in each cell, which will be a building block for the guidelines of the cellular design.

Notation: $\mathbb{E}[\cdot]$ denotes the expectation operator, $f_x(\cdot)$ is the probability density function (pdf) of a continuous random variable x or the pmf of a discrete random variable x , $\mathcal{L}_x(\cdot)$ is the Laplace transform of the pdf of x , $B(\cdot, \cdot)$ is a beta function, $\gamma(\cdot, \cdot)$ is a lower incomplete gamma function, and ${}_1F_1(\cdot; \cdot; \cdot)$ or ${}_2F_1(\cdot, \cdot; \cdot; \cdot)$ is a hypergeometric function.

II. SYSTEM MODEL

The uplink cellular network to be analyzed consists of BSs, users, and schedulers. All of the following assumptions can be found in representative studies in which uplink cellular networks are analyzed [7], [8], except the assumptions that truncated fractional power control per user [8], [23] and channel-adaptive user scheduling [15], [17] are performed.

The locations of the BSs and users form independent PPPs in \mathbb{R}^2 with the respective intensities, λ_{BS} and λ_{UE} , as in [25], [26]. The PPP assumption is widely accepted as the baseline assumption for a cellular system analysis [3], [5]. Note that the performance gap between the PPP and actual distribution can be found in [5]. Each user is associated with the nearest BS, meaning that the cell of each BS comprises a Voronoi tessellation on a plane.

We assume that a single resource block exists in the frequency domain. Note that for the case of multiple resource blocks in the frequency domain, the analysis for each resource

block reduces to an analysis with a single resource block by assuming independence among the resource blocks.

We assume that the desired and interference signals experience a path loss with a path loss exponent η and quasi-static Rayleigh fading (i.e., the channel gain is constant over a time slot and is exponentially distributed with a mean of 1).

Although the system model presented in this paper for uplink cellular networks is based on many aspects of that presented in [8], two essential differences exist: we consider the channel-adaptive user scheduling in which a transmitting user is selected according to the aforementioned manner, whereas a transmitting user is randomly chosen in [7], [8], and we consider cells that include no transmitting user. By contrast, in [8], the locations of users are arranged such that each BS has at least one scheduled user. As a result, in this study the density of interfering users is reduced.

A. Transmission Power Control

We assume that each user adjusts its transmit power according to truncated fractional power control. In this system, each user transmits according to the following two rules.

As the first rule, **(P1)**, a user within $R_d := (P_M/\rho_o)^{1/\eta\epsilon}$ from the serving BS transmits at transmit power $r^{\eta\epsilon}\rho_o$, where P_M is the maximum transmit power, $\epsilon \in [0, 1]$ is a power control factor, r is a contact distance, and ρ_o is a constant. Note that R_d is the distance over which a radio signal transmitted at the maximum transmit power P_M from a user decays to the constant ρ_o on average. Note that the transmit power control in this study is a generalization of that given in [7], [8], in which uplink cellular networks were analyzed by means of stochastic geometry. The case in which $\epsilon = 1$, namely, when the factor relative to the contact distance r disappears from the product of transmit power $r^{\eta}\rho_o$ and distance attenuation $r^{-\eta}$ (i.e., *perfect channel inversion* is achieved), was analyzed in [8], and the case in which $P_M \rightarrow \infty$, namely, when no maximum power constraint exists, was analyzed in [7].

The second rule is for the users outside the range of R_d (hereinafter referred to as *edge users* for simplicity) in each Voronoi cell. Note that the term “edge user” does not necessarily mean a user with poor communication quality in this context; this type of usage can also be found in [8]. We can consider how to treat edge users in two ways: **(P2a)**, where an edge user is not allowed to transmit, and **(P2b)**, where an edge user transmits at the maximum transmit power. In previous studies, the rules (P2a) and (P2b) are used separately: (P2a) can be found in [8] and (P2b) in [7], [23], [27], [28]. Note that, although rule (P2a) does not ensure fairness among users, edge users transmitting at the maximum transmit power can significantly increase the interference in the system and thus degrade the network performance [8], which motivated us to consider rule (P2a). We start by describing the case with (P1) and (P2a) in Section III-A and then extend it to the case with (P1) and (P2b) in Section III-D. Note that considering the probability of no BS existing within R_d based on the definition of PPP [2], the fraction of edge users is given by $e^{-\pi\lambda_{\text{BS}}R_d^2}$, which is found in several parts of this paper, including Sections III-B and III-D.

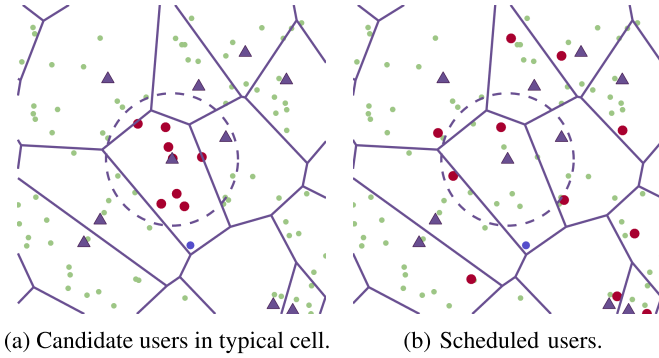


Fig. 1. Red dots represent each type of user, the dashed circle represents the achievable range (see Section III-B), purple triangles represent BSs, green dots represent users, and blue circles represent edge users in a typical cell.

B. Normalized SNR-Based Scheduler

In our system model, a scheduler selects the user to transmit in each time slot. Each BS is assumed to have knowledge of the instantaneous SNRs of the candidate users according to the channel estimation at the beginning of each time slot. Note that we discuss the SINR analysis with perfect CSI in Section III, and then discuss the SINR analysis with imperfect CSI in Section IV. We consider the normalized SNR-based scheduler [15], [17], which selects the user with the largest instantaneous SNR normalized by the *short-term* average SNR in each time slot. Given the fading gain h_i , transmit power p_i , and distance to the serving BS (i.e., *contact distance*) r_i of user i , the normalized SNR of user i is obtained as follows.

$$\frac{SNR_i}{\mathbb{E}_{h_i}[SNR_i]} = \frac{h_i p_i r_i^{-n} / \sigma_i^2}{\mathbb{E}_{h_i}[h_i p_i r_i^{-n} / \sigma_i^2]} = h_i$$

The short-term average SNR is the average value of the instantaneous SNR over a period during which the variation in the contact distance (as well as transmit power) is negligible. Note that if the data rate is proportional to the SNR [20], the normalized SNR-based scheduler is equivalent to the proportional fair scheduler [14].

As shown in the previous equation, this scheduler selects the user having the largest fading gain among all candidate users [15], [16], whereas the round-robin scheduler selects a user regardless of the channel conditions. A user currently selected to transmit in each cell is referred to as a *scheduled user*. Fig. 1 presents the definitions of candidate users and scheduled users to clarify the difference between them. Note that the authors of [15] considered a downlink analysis with the same scheduler, whereas in the present study we address an uplink analysis with truncated fractional power control.

III. SINR CCDF AND AVERAGE DATA RATE FOR PERFECT CSI AND SINGLE-USER-SINGLE-RESOURCE-BLOCK CASE

In this section, we describe the acquisition of the SINR ccdf and the average data rate for the uplink system. The SINR ccdf of a typical scheduled user is the probability that the user achieves a target value θ of the SINR when it is scheduled, which is defined as $\bar{F}_{SINR}(\theta) := \mathbb{P}(SINR > \theta)$.

In this section, as a basic scenario, we assume that the perfect CSI is available for schedulers and that at most one user is allowed to transmit in each resource block (or time slot). In this case, the scheduler always selects the user with the largest fading gain to be scheduled and does not select the other candidate users. We extend the framework to handle the basic scenario in this section to the case of assigning a single resource block to multiple users and the case of imperfect CSI in Section IV.

We first introduce the SINR with truncated fractional power control. Without loss of generality, we can assume that a typical BS is located at the origin. The SINR relative to the typical scheduled user is denoted by:

$$SINR = \frac{\max_{i=1,2,\dots,n} h_i r_i^{\eta(\epsilon-1)} \rho_o}{\sigma^2 + I}, \quad (1)$$

where h_i is the fading gain of candidate user i exponentially distributed with a mean of 1, r is the contact distance of a typical scheduled user, and n represents the number of candidate users in the associated cell. The max operator reflects the fact that the scheduler selects the user with the largest fading gain. Note that the power control is assumed to be performed in advance of the scheduling. The parameter σ^2 denotes the noise power, and the value I is the aggregate interference power defined as:

$$I = \sum_{u \in \Phi_{su} \setminus \{u_o\}} g_u p_u \|u\|^{-\eta}, \quad (2)$$

where Φ_{su} is a point process formed by the locations of scheduled users, and u_o is a typical scheduled user. The parameters g_u and p_u represent the fading gain and the transmit power relative to interfering user $u \in \Phi_{su} \setminus \{u_o\}$, respectively.

In normalized SNR-based scheduling, the fading gain of a typical scheduled user follows the distribution of the largest order statistic [18] for the given fading gains of the involved users in the corresponding cell [15]. The distribution is given by:

$$\mathbb{P}\left(\max_{i=1,2,\dots,n} h_i \leq x\right) = (1 - e^{-x})^n. \quad (3)$$

The aforementioned distribution also appears in the calculation of the selection combiner output [29]. However, unlike in selection combining, n is a random variable because of the inherent randomness of the positions of the BSs and users in Poisson cellular networks.

We now state the main results of this study. Before deriving the SINR ccdf in a complete form, we can give the general results by utilizing the fact that the multi-user diversity gain increases with the number of candidate users in the corresponding cell. Letting the number of candidate users be a random variable n , we obtain:

$$\begin{aligned} \bar{F}_{SINR}(\theta) &= \mathbb{E}_n[\mathbb{P}(SINR > \theta | n) | n > 0] \\ &= \sum_{n=1}^{\infty} \frac{f_n(n)}{1 - f_n(0)} \mathbb{P}(SINR > \theta | n), \end{aligned} \quad (4)$$

where $\mathbb{P}(SINR > \theta | n)$ denotes the SINR ccdf conditional on n and $f_n(n)$ is the pmf of the number of candidate users in

each cell. Note that we do not focus on the cells that include no candidate users because $\mathbb{P}(\text{SINR} | n = 0)$ is unreasonable, and thus we average over the distribution conditioned on $n > 0$. To simplify the notation of conditional expectation given $n > 0$, we use the notation $\mathbb{E}_{n>0}[\cdot] := \mathbb{E}_n[\cdot | n > 0]$. We first present the derivation of $\mathbb{P}(\text{SINR} > \theta | n)$ (see Lemma 1), as well as some simpler expressions in Section III-A. We then discuss the details of the number distribution of candidate users in Section III-B.

A. Conditional SINR cdf Given Number of Candidate Users

Before deriving the SINR cdf, we make three approximations for analytical tractability. We assume that the number of candidate users n and the contact distance r are independent, the scheduled users form a PPP with intensity λ_{BS} , and the transmit powers of the scheduled users are independent. The first assumption was employed in [15], and the last two approximations were employed in [8], each of which showed that the approximations maintain the accuracy of the leading results. The validation of the approximations is also shown through a numerical evaluation described in Section V. Note that the assumption that the PPP formed by all users (not scheduled users) is independent of the PPP formed by BSs, as given in Section II, is not used in deriving the conditional SINR cdf given the number of candidate users, but instead contributes to obtaining the pmf of the number of candidate users in each cell, as described in Section III-B.

As the maximum contact distance is thought to be R_d , the contact distance follows the following truncated Rayleigh distribution:

$$f_r(r) = z_r^{-1} r e^{-\pi \lambda_{\text{BS}} r^2} \mathbb{1}_{\{0 \leq r \leq R_d\}}, \quad (5)$$

where z_r^{-1} is a normalizing constant and $\mathbb{1}_{\{\text{condition}\}}$ is the indicator function, which equals 1 if *condition* is true and zero otherwise. Note that the unrestricted case (i.e., $R_d \rightarrow \infty$) corresponds to a Rayleigh distribution, which is the standard assumption concerning the contact distance in a cellular analysis [2], [5]. By considering the distribution of a transformed variable $p = r^{\eta\epsilon} \rho_o$, we derive the distribution of the transmit powers of interfering users as:

$$f_p(p) = z_p^{-1} p^{\frac{2}{\eta\epsilon} - 1} e^{-\pi \lambda_{\text{BS}} \left(\frac{p}{\rho_o}\right)^{\frac{2}{\eta\epsilon}}} \mathbb{1}_{\{0 \leq p \leq P_M\}}, \quad (6)$$

where z_p^{-1} is a normalizing constant.

Lemma 1: Suppose n and r are independent, Φ_{su} is independent of the PPP formed by BSs, and the transmit powers of scheduled users are independent. $\mathbb{P}(\text{SINR} > \theta | n)$ is given by:

$$\begin{aligned} \mathbb{P}(\text{SINR} > \theta | n) &= \sum_{k=1}^n \binom{n}{k} (-1)^{k+1} \mathbb{E}_r \\ &\times \left[\exp \left(-\frac{k\theta\sigma^2}{r^{\eta(\epsilon-1)}\rho_o} - \frac{2\pi k\theta\lambda_{\text{BS}}r^{2-\eta\epsilon}}{(\eta-2)/(1-f_n(0))} \right) \mathbb{E}_p \right. \\ &\times \left. \left[p {}_2F_1 \left(1, 1 - \frac{2}{\eta}; 2 - \frac{2}{\eta}; -\frac{k\theta p}{r^{\eta\epsilon}\rho_o} \right) \right] \right]. \quad (7) \end{aligned}$$

Proof: We have:

$$\begin{aligned} \mathbb{P}(\text{SINR} > \theta | n) &= \mathbb{E}_{r,I} [\mathbb{P}(\text{SINR} > \theta | n, r, I)] \\ &= \mathbb{E}_{r,I} \left[\mathbb{P} \left(\frac{\max_{i=1,2,\dots,n} h_i r^{\eta(\epsilon-1)} \rho_o}{\sigma^2 + I} > \theta \mid n, r, I \right) \right] \\ &= \mathbb{E}_{r,I} \left[\mathbb{P} \left(\max_{i=1,2,\dots,n} h_i > \frac{\theta(\sigma^2 + I)}{r^{\eta(\epsilon-1)} \rho_o} \mid n, r, I \right) \right] \\ &= \mathbb{E}_{r,I} \left[1 - \left(1 - \exp \left(-\frac{\theta(\sigma^2 + I)}{r^{\eta(\epsilon-1)} \rho_o} \right) \right)^n \right] \\ &= \mathbb{E}_{r,I} \left[\sum_{k=1}^n \binom{n}{k} (-1)^{k+1} \exp \left(-\frac{k\theta(\sigma^2 + I)}{r^{\eta(\epsilon-1)} \rho_o} \right) \right] \quad (8) \\ &= \sum_{k=1}^n \binom{n}{k} (-1)^{k+1} \mathbb{E}_r \left[e^{-\frac{k\theta\sigma^2}{r^{\eta(\epsilon-1)}\rho_o}} \mathbb{E}_I \left[e^{-\frac{k\theta I}{r^{\eta(\epsilon-1)}\rho_o}} \right] \right] \\ &= \sum_{k=1}^n \binom{n}{k} (-1)^{k+1} \mathbb{E}_r \left[e^{-\frac{k\theta\sigma^2}{r^{\eta(\epsilon-1)}\rho_o}} \mathcal{L}_I \left(\frac{k\theta}{r^{\eta(\epsilon-1)}\rho_o} \right) \right]. \quad (9) \end{aligned}$$

Note that $\mathbb{P}(\text{SINR} > \theta | n, r)$ is given based on the expectation of the sum of the exponential functions of interference I in (8) because the distribution of the fading gain of the scheduled user (3) can be written as the sum of the exponential functions according to the binomial theorem. Although this property is true for the downlink analysis [15], the element regarding the Laplace transform is different because of the power control and the difference in the interference sources.

The remainder of the proof is given in Appendix A. \square

Considering $p = r^{\eta\epsilon} \rho_o$, we can see that the average over p is equivalent to that over r . The conditional SINR distribution given that the number of candidate users is fixed at one, i.e., $\mathbb{P}(\text{SINR} > \theta | n = 1)$, corresponds to the analysis given in [7], which does not consider channel-adaptive user scheduling but rather round-robin scheduling.

For the interference-limited case (i.e., $\sigma^2 + I \simeq I$), the first exponential function in (7) can be ignored. When $\eta = 4$, the hypergeometric function reduces by ${}_2F_1(1, 1/2; 3/2; -x) = \sqrt{x} \arctan \sqrt{x}$. The assumption of the previous two conditions yields a simpler expression:

$$\begin{aligned} \mathbb{P}(\text{SINR} > \theta | n) &= \sum_{k=1}^n \binom{n}{k} (-1)^{k+1} \\ &\times \mathbb{E}_r \left[\exp \left(-\pi \lambda_{\text{BS}} (1 - f_n(0)) r^2 \right) \mathbb{E}_p \right. \\ &\times \left. \left[\sqrt{\frac{k\theta p}{r^{4\epsilon}\rho_o}} \arctan \sqrt{\frac{k\theta p}{r^{4\epsilon}\rho_o}} \right] \right]. \end{aligned}$$

Corollary 1: Suppose $\epsilon = 1$ (i.e., when perfect channel inversion is achieved), we can simplify the SINR cdf

conditional on n as:

$$\mathbb{P}(SINR > \theta | n) = \sum_{k=1}^n \binom{n}{k} (-1)^{k+1} \exp\left(-\frac{k\theta\sigma^2}{\rho_o}\right) \times \exp\left(-\frac{2k\theta\gamma(2, \pi\lambda_{BS}R_d^2)}{(\eta-2)(1-e^{-\pi\lambda_{BS}R_d^2})/(1-f_n(0))}\right). \quad (10)$$

Proof: See Appendix B. \square

Note that $\mathbb{P}(SINR > \theta | n = 1, \epsilon = 1)$ corresponds to the same analysis given in [8] except that the density of interfering users is reduced to $(1 - f_n(0))\lambda_{BS}$ because of the absence of users in certain cells. It should also be noted that for $\epsilon = 1$, we can drop the random variable r in the analysis, and thus we no longer require the assumption of independence between n and r , which is assumed in Lemma 1. Whereas the accuracy of these approximations was validated in [8] for the case without channel-adaptive scheduling, in Section V it is validated for a case in which channel-adaptive scheduling is employed.

Simpler expressions can be derived for certain special cases. For the interference-limited case, $\exp(-k\theta\sigma^2/\rho_o)$ can be ignored. When $\eta = 4$, the part related to the hypergeometric function reduces to the closed-form expression, $\sqrt{k\theta} \arctan(\sqrt{k\theta})$. In the case of $P_M \rightarrow \infty$ (equivalently $R_d \rightarrow \infty$), $\gamma(2, \pi\lambda_{BS}R_d^2)$ reduces to 1 and $1 - e^{-\pi\lambda_{BS}R_d^2} \rightarrow 1$. The simplest form is obtained when the previous three conditions are simultaneously satisfied, which leads to

$$\mathbb{P}(SINR > \theta | n) = \sum_{k=1}^n \binom{n}{k} (-1)^{k+1} e^{-(1-f_n(0))\sqrt{k\theta} \arctan \sqrt{k\theta}}. \quad (11)$$

Note that the previous expression is a closed form and depends only on a threshold θ . We should also note that allowing the number of candidate users n to be 1 with probability 1 corresponds to the results of typical uplink analyses [7], [8], and thus our results are a natural extension of them to a case in which an active user is not randomly selected.

B. Number Distribution of Candidate Users

The derivation of the SINR cdf is complete if we have the number distribution of candidate users in each cell, $f_n(n)$. In fact, the distribution depends on the existing range of a scheduled user. To discuss the existing range, we define the achievable range of the BS as the circle centered in a typical BS with radius R_d . The users outside the achievable range of the serving BS are not allowed to transmit frames owing to the maximum power constraint.

In this section, we first provide the distribution for two asymptotic cases, where the achievable range relative to the typical BS includes the corresponding Voronoi cell, as shown in Fig. 2(a), with a high probability, and where the typical Voronoi cell includes the corresponding achievable range, as shown in Fig. 2(c), with a high probability. Next, we give a general distribution, which is more complicated than the former two distributions but is correct regardless of the manner in which a Voronoi cell and the corresponding achievable range overlap.

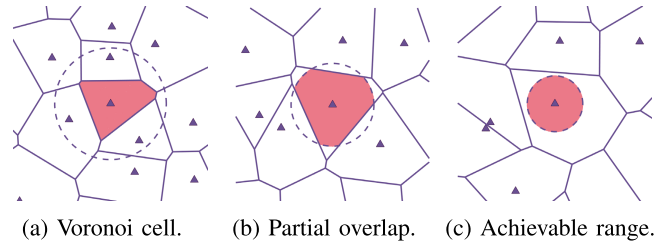


Fig. 2. Existing range of scheduled user. The red region represents the existing range, the dashed circle represents the achievable range with radius R_d , and the purple triangles represent BSs.

With respect to a typical BS, the existing range corresponds to the Voronoi cell, as shown in Fig. 2(a), with probability

$$g_1(\lambda_{BS}, R_d) = 1 - e^{-\pi\lambda_{BS}R_d^2}, \quad (12)$$

which is equivalent to the probability that at least one BS exists within R_d of a certain user. By contrast, the existing range corresponds to the achievable range, as shown in Fig. 2(c), with probability

$$g_2(\lambda_{BS}, R_d) = e^{-4\pi\lambda_{BS}R_d^2}, \quad (13)$$

which is equivalent to the probability that no cell edges exist within R_d from the BS, namely, the probability that no other BS exists within the circle centered at the typical BS with radius $2R_d$. Therefore, the case shown in Fig. 2(b) occurs with probability $1 - g_1 - g_2$.

Given area a of the corresponding existing range in a typical cell, the pmf of the number of involved users is given by:

$$f_n | a(n | a) = \frac{(\lambda_{UE}a)^n}{n!} e^{-\lambda_{UE}a}, \quad (14)$$

from the definition of PPP [2]. Therefore, if given the distribution $f_a(a)$ of area a of the existing range in a typical cell, we can obtain the number distribution of candidate users by

$$f_n(n) = \int_0^\infty f_n | a(n | a) f_a(a) da. \quad (15)$$

1) *Asymptotic Cases:* If $g_1(\lambda_{BS}, R_d) \simeq 1$, $f_a(a)$ corresponds to the distribution of the area of the typical Voronoi cell, and the corresponding distribution of the candidate users is given, as in [25], we can obtain:

$$f_n^{(1)}(n) = \frac{(\lambda_{UE}/c\lambda_{BS})^n}{cB(n+1, c-1)(\lambda_{UE}/c\lambda_{BS} + 1)^{n+c}}, \quad c = 3.5. \quad (16)$$

If $g_2(\lambda_{BS}, R_d) \simeq 1$, area a equals πR_d^2 with probability one, and therefore the number distribution of candidate users is given by:

$$f_n^{(2)}(n) = \frac{(\lambda_{UE}\pi R_d^2)^n}{n!} e^{-\lambda_{UE}\pi R_d^2}. \quad (17)$$

Substituting (7) and (16) or (17) into (4), we obtain (18), shown at the bottom of the next page, and the following proposition.

Proposition 1: The SINR cdf $\bar{F}_{SINR}(\theta)$ of the normalized SNR-based scheduling in uplink cellular networks is given by (18), which is appropriate if $g_i(\lambda_{BS}, R_d) \simeq 1$ ($i = 1, 2$).

Corollary 2: Suppose that $\epsilon = 1$ (i.e., perfect channel inversion is performed). The SINR ccdf $\bar{F}_{SINR}(\theta)$ of the normalized SNR-based scheduling in uplink cellular networks is given by (19), shown at the bottom of this page, which is appropriate if $g_i(\lambda_{BS}, R_d) \simeq 1$ ($i = 1, 2$).

2) *General Case:* In this section, we provide the pmf of n , which is always applicable regardless of λ_{BS} and R_d . To obtain the pmf of n , we consider two facts regarding the area distribution $f_a(a)$. First, because of the restriction of the achievable range, it is necessary that area a of the existing range in a typical cell be distributed over $[0, \pi R_d^2]$. Second, an achievable range is included in the corresponding Voronoi cell with probability $g_2(\lambda_{BS}, R_d)$, and thus, $f_a(\pi R_d^2) = g_2(\lambda_{BS}, R_d)\delta(a - \pi R_d^2)$, where $\delta(a)$ is the Dirac delta function. In this sense, $g_2(\lambda_{BS}, R_d)$ can be interpreted as the degree to which the distribution is concentrated around $a = \pi R_d^2$. Because of its flexibility and boundedness [23], [30], we use the beta distribution to model the distribution of the area of the existing range in a typical cell over $[0, \pi R_d^2]$. As the beta distribution is defined over $[0, 1]$, considering the distribution of the normalized area $\hat{a} = a/\pi R_d^2$, we have a parametric model

$$f_{\hat{a}}(a) = (1 - g_2) \frac{a^{\alpha-1}(1-a)^{\beta-1}}{B(\alpha, \beta)} + g_2\delta(a-1). \quad (20)$$

Parameters α and β are determined as the functions of λ_{BS} and R_d through the following two steps. First, we obtain the fitted parameters for certain values of λ_{BS} through Monte Carlo simulations, followed by the generalized representations of the parameters as functions of λ_{BS} and R_d through a piecewise linear approximation. Note that the derivation of (16) requires the distribution of the area of a typical Voronoi cell, which is also identified by parameter fitting through Monte Carlo simulations [31]. Fig. 3 shows the parameter estimates obtained by means of Monte Carlo simulations and the corresponding fitted curves, which are given by:

$$\log \alpha = \begin{cases} 1.3 \log(\lambda_{BS} R_d^2) + 9.72, & 5.36 \times 10^{-2} < \lambda_{BS} R_d^2; \\ 0.9, & \text{otherwise.} \end{cases}$$

$$\log \beta = \begin{cases} -0.96 \log(\lambda_{BS} R_d^2) - 7.74, & 6.7 \times 10^{-2} > \lambda_{BS} R_d^2; \\ -1.6, & \text{otherwise.} \end{cases}$$

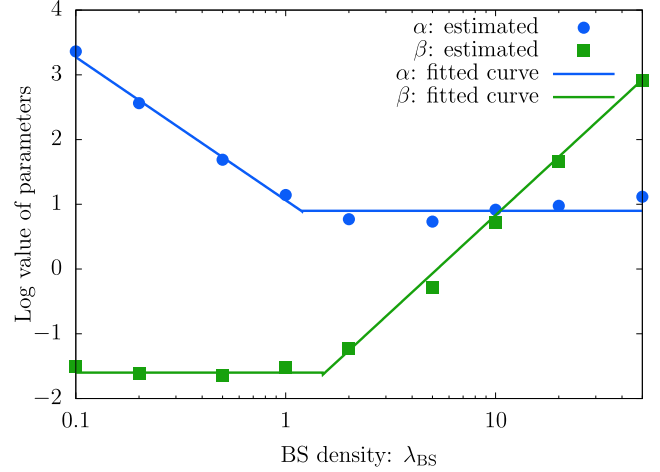


Fig. 3. Parameters of a beta distribution. The points represent fitted parameters through Monte Carlo simulations, and the lines represent generalized representations of the parameters as functions of λ_{BS} ($\rho_o = -70$ dB).

Note that the parameters depend on λ_{BS} and R_d through $\lambda_{BS} R_d^2$, because the degree to which the distribution is concentrated around $a = \pi R_d^2$ is determined based on $g_2(\lambda_{BS}, R_d)$ and thus by $\lambda_{BS} R_d^2$.

Substituting (14) and (20) into (15), we obtain (21), shown at the bottom of this page. Therefore, we can derive the following proposition, which holds for any λ_{BS} and R_d .

Proposition 2: The SINR ccdf $\bar{F}_{SINR}(\theta)$ of the normalized SNR-based scheduling in an uplink cellular network is given by letting $i = 3$ in (18).

Corollary 3: Suppose that $\epsilon = 1$ (i.e., perfect channel inversion is performed). The SINR ccdf $\bar{F}_{SINR}(\theta)$ of the normalized SNR-based scheduling in an uplink cellular network is given by letting $i = 3$ in (19).

C. Average Data Rate

Using the SINR ccdf, we can obtain the average data rate $\tau_s(\lambda_{BS}, \lambda_{UE}) := \mathbb{E}[\ln(1 + SINR)]$, and therefore, the scheduling gain [32] $G(\lambda_{BS}, \lambda_{UE}) := \tau_s(\lambda_{BS}, \lambda_{UE})/\tau_r(\lambda_{BS})$, where $\tau_r(\lambda_{BS})$ is the average data rate of the round-robin scheduling,

$$\bar{F}_{SINR}(\theta) = \sum_{n=1}^{\infty} \frac{f_n^{(i)}(n)}{1 - f_n^{(i)}(0)} \sum_{k=1}^n \binom{n}{k} (-1)^{k+1} \mathbb{E}_r \left[\exp \left(-\frac{k\theta\sigma^2}{r\eta(\epsilon-1)\rho_o} - \frac{2\pi k\theta\lambda_{BS}r^{2-\eta\epsilon}}{(\eta-2)/(1-f_n^{(i)}(0))} \mathbb{E}_p \left[p_2 F_1 \left(1, 1 - \frac{2}{\eta}; 2 - \frac{2}{\eta}; -\frac{k\theta p}{r\eta\epsilon} \right) \right] \right) \right]. \quad (18)$$

$$\bar{F}_{SINR}(\theta) = \sum_{n=1}^{\infty} \frac{f_n^{(i)}(n)}{1 - f_n^{(i)}(0)} \sum_{k=1}^n \binom{n}{k} (-1)^{k+1} \exp \left(-\frac{k\theta\sigma^2}{\rho_o} - \frac{2k\theta\gamma(2, \pi\lambda_{BS}R_d^2)}{(\eta-2)(1 - e^{-\pi\lambda_{BS}R_d^2})/(1 - f_n^{(i)}(0))} {}_2F_1 \left(1, 1 - \frac{2}{\eta}; 2 - \frac{2}{\eta}; -k\theta \right) \right), \quad (19)$$

$$\begin{aligned} f_n^{(3)}(n) &= \int_0^1 \frac{(\lambda_{UE}\pi R_d^2 a)^n}{n!} e^{-\lambda_{UE}\pi R_d^2 a} f_{\hat{a}}(a) da \\ &= (1 - g_2) \frac{B(n + \alpha, \beta)}{B(\alpha, \beta)} \frac{(\lambda_{UE}\pi R_d^2)^n}{n!} \int_0^1 \frac{a^{n+\alpha-1}(1-a)^{\beta-1}}{B(n + \alpha, \beta)} e^{-\lambda_{UE}\pi R_d^2 a} da + g_2 \frac{(\lambda_{UE}\pi R_d^2)^n}{n!} e^{-\lambda_{UE}\pi R_d^2} \\ &= (1 - g_2) \frac{B(n + \alpha, \beta)}{B(\alpha, \beta)} \frac{(\lambda_{UE}\pi R_d^2)^n}{n!} {}_1F_1(n + \alpha; n + \alpha + \beta; -\lambda_{UE}\pi R_d^2) + g_2 \frac{(\lambda_{UE}\pi R_d^2)^n}{n!} e^{-\lambda_{UE}\pi R_d^2}. \end{aligned} \quad (21)$$

which is given as:

$$\tau_r(\lambda_{BS}) = \int_0^\infty \frac{e^{-\frac{x\sigma^2}{\rho_o}}}{x+1} \mathcal{L}_I\left(\frac{x}{\rho_o}\right) dx. \quad (22)$$

Note that these average data rates are not defined for cells in which no scheduled users exist. Also note that (22) differs from that presented in [8] in that we consider BSs as having no users to serve.

Corollary 4: The average data rate $\tau_s(\lambda_{BS}, \lambda_{UE})$ of the normalized SNR-based scheduling is given by:

$$\mathbb{E}_{n>0} \left[\sum_{k=1}^n \binom{n}{k} (-1)^{k+1} \mathbb{E}_r \left[\int_0^\infty \frac{e^{-\frac{kx\sigma^2}{\rho_o r^\eta(\epsilon-1)}}}{x+1} \mathcal{L}_I\left(\frac{kx}{\rho_o r^\eta(\epsilon-1)}\right) dx \right] \right]. \quad (23)$$

In particular, letting $\sigma^2 = 0$, $P_M \rightarrow \infty$, $\eta = 4$, $\epsilon = 1$ yields a simpler form:

$$\mathbb{E}_{n>0} \left[\sum_{k=1}^n \binom{n}{k} (-1)^{k+1} \int_0^\infty \frac{e^{-(1-f_n^{(i)}(0))\sqrt{kx} \arctan(\sqrt{kx})} dx}{x+1} \right]. \quad (24)$$

Proof: See Appendix C. \square

D. Analysis with Edge Users

The aforementioned analyses were conducted by focusing on users within an achievable range, where the edge users are not allowed to transmit. We now consider the extension of the aforementioned framework to the case in which edge users are permitted to transmit at the maximum transmit power P_M .

We introduce s_{in} supposed on $\{0, 1\}$ as a variable indicating whether a typical scheduled user is located within an achievable range. As the proportion of edge users is given by $1 - g_1(\lambda_{BS}, R_d)$ in a Poisson cellular network, Here, $s_{in} = 1$ means the user is inside the achievable range, whereas $s_{in} = 0$ means the user is an edge user. we have $\mathbb{P}(s_{in} = 1) = g_1(\lambda_{BS}, R)$ and $\mathbb{P}(s_{in} = 0) = 1 - g_1(\lambda_{BS}, R_d)$.

The SINR cdf conditional on $s_{in} = 1$ is the same as (9) except for the distribution of transmit power of an interfering user. Within the entire network, a fraction $1 - g_1(\lambda_{BS}, R)$ of

users transmit according to the fractional power control, and a fraction $g_1(\lambda_{BS}, R)$ transmits at the maximum transmit power. Thus, the distribution of transmit power of an interfering user is given as:

$$f_{\hat{p}}(p) = g_1 z_p^{-1} p^{\frac{2}{\eta\epsilon}-1} e^{-\pi\lambda_{BS}\left(\frac{p}{\rho_o}\right)^{\frac{2}{\eta\epsilon}}} \mathbb{1}_{\{0 \leq p < P_M\}} + (1 - g_1)\delta(p - P_M) \mathbb{1}_{\{p=P_M\}}. \quad (25)$$

The SINR cdf conditional on $s_{in} = 0$ is given by replacing $r^\eta \rho_o$ with P_M in (9):

$$\begin{aligned} & \mathbb{P}(SINR > \theta | s_{in} = 0) \\ &= \mathbb{E}_{n>0} \left[\sum_{k=1}^n \binom{n}{k} (-1)^{k+1} \right. \\ & \quad \left. \times \mathbb{E}_{\hat{r}} \left[\exp\left(-\frac{k\theta\sigma^2}{P_M \hat{r}^{-\eta}}\right) \mathcal{L}_I\left(\frac{k\theta}{P_M \hat{r}^{-\eta}}\right) \right] \right], \end{aligned} \quad (26)$$

where r' is a contact distance of an edge user, which follows the Rayleigh distribution truncated in (R_d, ∞) :

$$f_{\hat{r}}(r) = z_{\hat{r}}^{-1} r e^{-\pi\lambda_{BS}r^2} \mathbb{1}_{\{r>R_d\}}, \quad (27)$$

where $z_{\hat{r}}^{-1}$ is a normalizing constant.

Averaging out the random variable s_{in} yields (28), shown at the bottom of this page. In this case, because every user can transmit, the number distribution of candidate users is given by $f_n^{(1)}(n)$, which is the number distribution of users in a typical Voronoi cell. Consequently, we have the following proposition.

Proposition 3: When edge users are allowed to transmit at the maximum transmit power, the SINR cdf $\bar{F}_{SINR}(\theta)$ of the normalized SNR-based scheduling in an uplink cellular network is given by (28).

IV. EXTENSION FOR MULTIPLE USER AND IMPERFECT CSI

In this section, we extend the aforementioned mentioned framework in two ways, that is, we consider the case in which multiple user are supported in a single resource block and the case in which perfect CSI is not available for schedulers. The two cases are related through the SINR analysis of a user with the i th largest fading gain in a cell.

$$\begin{aligned} \mathbb{P}(SINR > \theta) &= \sum_{i \in \{0,1\}} \mathbb{P}(SINR > \theta | s_{in} = i) \mathbb{P}(s_{in} = i) \\ &= \mathbb{E}_{n>0} \left[\sum_{k=1}^n \binom{n}{k} (-1)^{k+1} \left\{ g_1 \mathbb{E}_r \left[e^{-\frac{k\theta\sigma^2}{r^\eta(\epsilon-1)\rho_o}} \mathcal{L}_I\left(\frac{k\theta}{r^\eta(\epsilon-1)\rho_o}\right) \right] \right. \right. \\ & \quad \left. \left. + (1 - g_1) \mathbb{E}_{\hat{r}} \left[e^{-\frac{k\theta\sigma^2}{P_M \hat{r}^{-\eta}}} \mathcal{L}_I\left(\frac{k\theta}{P_M \hat{r}^{-\eta}}\right) \right] \right\} \right] \\ &= \sum_{n=1}^{\infty} \frac{f_n^{(1)}(n)}{1 - f_n^{(1)}(0)} \left[\sum_{k=1}^n \binom{n}{k} (-1)^{k+1} \left\{ g_1 \mathbb{E}_r \left[e^{-\frac{k\theta\sigma^2}{r^\eta(\epsilon-1)\rho_o}} \mathcal{L}_I\left(\frac{k\theta}{r^\eta(\epsilon-1)\rho_o}\right) \right] \right. \right. \\ & \quad \left. \left. + (1 - g_1) \mathbb{E}_{\hat{r}} \left[e^{-\frac{k\theta\sigma^2}{P_M \hat{r}^{-\eta}}} \mathcal{L}_I\left(\frac{k\theta}{P_M \hat{r}^{-\eta}}\right) \right] \right\} \right]. \end{aligned} \quad (28)$$

A. Discussion on Multiple Users

Considering multiple orthogonal resource blocks in the frequency domain, we can consider multiple users to be scheduled in each time slot. In this case, the SINR analysis in each resource block is reduced to the analysis under the single-user-single-resource-block assumption.

On the other hand, multiple users can also be supported in the same resource block by using space division multiple access [29] or non-orthogonal multiple access [33]. In that case, the normalized SNR-based scheduler selects a specified number of users to be scheduled in order of their fading gains.

In this section, we mainly give the conditional SINR ccdf relative to the user with the i th largest fading gain in a cell given the number of candidate users n . After that, we briefly explain the derivation of the SINR ccdf averaged over n and the average data rate because the corresponding processes are almost the same as in the single-user-single-resource block case.

We assume that the perfect CSI is available for schedulers in this subsection. Let $h_{(i,n)}$ be the i th largest of the fading gains h_1, h_2, \dots, h_n of candidate users (i.e., $h_{(1,n)} \geq h_{(2,n)} \geq \dots \geq h_{(n,n)}$). The distribution of the i th largest fading gain $h_{(i,n)}$ is given by

$$\begin{aligned} \mathbb{P}(h_{(i,n)} \leq x) &= \sum_{j=n-i+1}^n \binom{n}{j} (1 - e^{-x})^j \cdot (e^{-x})^{n-j} \\ &= \sum_{j=n-i+1}^n \binom{n}{j} \sum_{k=0}^j \binom{j}{k} (-1)^k e^{-(n+k-j)x}. \end{aligned} \quad (29)$$

Letting the SINR relative to the users with fading gain $h_{(i,n)}$ be denoted by $SINR_{(i,n)}$, we obtain

$$\begin{aligned} \mathbb{P}(SINR_{(i,n)} > \theta | n) &= \mathbb{E}_{r,I} \left[\mathbb{P} \left(\frac{h_{(i,n)} r^{\eta(\epsilon-1)} \rho_o}{\sigma^2 + I} > \theta \mid n, r, I \right) \right] \\ &= \mathbb{E}_{r,I} \left[\mathbb{P} \left(h_{(i,n)} > \frac{\theta(\sigma^2 + I)}{r^{\eta(\epsilon-1)} \rho_o} \mid n, r, I \right) \right] \\ &= \mathbb{E}_{r,I} \left[1 - \sum_{j=n-i+1}^n \binom{n}{j} \sum_{k=0}^j \binom{j}{k} (-1)^k \right. \\ &\quad \left. \exp \left(-\frac{(n+k-j)\theta(\sigma^2 + I)}{r^{\eta(\epsilon-1)} \rho_o} \right) \right] \end{aligned}$$

$$\begin{aligned} &= 1 - \sum_{j=n-i+1}^n \binom{n}{j} \sum_{k=0}^j \binom{j}{k} (-1)^k \cdot \\ &\quad \mathbb{E}_r \left[e^{-\frac{(n+k-j)\theta\sigma^2}{r^{\eta(\epsilon-1)} \rho_o}} \mathcal{L}_I \left(\frac{(n+k-j)\theta}{r^{\eta(\epsilon-1)} \rho_o} \right) \right]. \end{aligned} \quad (30)$$

Noticing that the Laplace transform of I is given by (35) in the same manner as Appendix A, we can obtain the analytical expression for $\mathbb{P}(SINR_{(i,n)} > \theta | n)$. Note that when applying the probability generation functional of PPP in the derivation of the Laplace transform of I , we need the density of interfering users, which is considered as $(1 - f_n(0))\lambda_{BS}$ in the previous section. However, if multiple users simultaneously transmit in a single resource block in each cell, the effective density of interfering users would be more than $(1 - f_n(0))\lambda_{BS}$ depending on a multiple access scheme. However, a detailed discussion on such an effective density is out of scope of this paper, and hence we just present a theoretical result as a form of lemma by letting the effective density of interfering users in a considered system be denoted by $\lambda_I^{(\text{eff})}$.

Lemma 2: Under the same assumptions as Lemma 1, the conditional SINR ccdf $\mathbb{P}(SINR_{(i,n)} > \theta | n)$ relative to the user with the i th largest fading gain is given by (31), shown at the bottom of this page.

Similar to the derivation of (11), letting $\sigma^2 = 0$, $P_M \rightarrow \infty$, $\eta = 4$, $\epsilon = 1$, we have a simpler form (32), shown at the bottom of this page. The only essential difference between (11) and (32) is that (32) includes one more finite summation than (11).

Averaging $\mathbb{P}(SINR_{(i,n)} > \theta | n)$ with respect to the number of candidate users n , we obtain the SINR ccdf $\mathbb{P}(SINR_{(i)} > \theta)$ relative to the user with the i th largest fading gain. Also, integrating $\mathbb{P}(SINR_{(i)} > e^t - 1)$ with respect to t from 0 to ∞ as in the single-user-single-resource-block case under the perfect CSI assumption, we obtain the average data rate. The process of averaging for n and that of obtaining the average data rate are the same as in Section III-B and in Appendix C, respectively.

B. Discussion on Imperfect CSI

Thus far we have assumed that the perfect CSI is available for schedulers. However, the perfect CSI is not necessarily available in a practical system. In this section, we consider the SINR distribution under the imperfect CSI assumption.

$$\begin{aligned} \mathbb{P}(SINR_{(i,n)} > \theta | n) &= 1 - \sum_{j=n-i+1}^n \binom{n}{j} \sum_{k=0}^j \binom{j}{k} (-1)^k \\ &\quad \times \mathbb{E}_r \left[\exp \left(-\frac{(n+k-j)\theta\sigma^2}{r^{\eta(\epsilon-1)} \rho_o} - \frac{2\pi(n+k-j)\theta\lambda_I^{(\text{eff})} r^{2-\eta\epsilon}}{(\eta-2)} \right) \right. \\ &\quad \left. \times \mathbb{E}_p \left[p_2 F_1 \left(1, 1 - \frac{2}{\eta}; 2 - \frac{2}{\eta}; -\frac{(n+k-j)\theta p}{r^{\eta\epsilon} \rho_o} \right) \right] \right]. \end{aligned} \quad (31)$$

$$\mathbb{P}(SINR_{(i,n)} > \theta | n) = 1 - \sum_{j=n-i+1}^n \binom{n}{j} \sum_{k=0}^j \binom{j}{k} (-1)^k \exp \left(-\frac{\lambda_I^{(\text{eff})}}{\lambda_{BS}} \sqrt{(n+k-j)\theta} \arctan \sqrt{(n+k-j)\theta} \right). \quad (32)$$

We consider the case in which a scheduler tries to assign a resource block to the user who has the largest fading gain in actual, as in Section III. Note that the case in which a scheduler tries to assign the same resource block to the user with the i th largest fading gain can be considered in the same manner as in the previous section. Under the imperfect CSI assumption, the scheduler observes the channel gains (equivalent to fading gains) of candidate users with noise. Let the fading gain of user i observed by the scheduler be denoted by \tilde{h}_i . In this system, a scheduler assigns a resource block to a user with fading gain $\max_{i=1,2,\dots,n} \tilde{h}_i$ in each time slot. Therefore, a user with fading gain $h_{(1,n)} = \max_{i=1,2,\dots,n} h_i$ is not necessarily scheduled in general.

We denote the probability that the scheduler assigns a resource block to the user with fading gain $h_{(i,n)}$ by $p_{(i,n)}^{\text{sche}}$, which depends on the observation model of fading gains. Note that under the perfect CSI assumption, $p_{(i,n)}^{\text{sche}} = 1$ for $i = 1$ and $p_{(i,n)}^{\text{sche}} = 0$ otherwise. Noticing that the SINR cdf for the user with fading gain $h_{(i,n)}$ is given in (31) or (32) (note that $\lambda_I^{\text{(eff)}}$ is $(1 - f_n(0))\lambda_{\text{BS}}$ for the single-user-single-resource-block case), we obtain the SINR cdf under the imperfect CSI assumption as follows.

$$\mathbb{P}(\text{SINR} > \theta | n) = \sum_{i=1}^n p_{(i,n)}^{\text{sche}} \cdot \mathbb{P}(\text{SINR}_{(i,n)} > \theta | n). \quad (33)$$

We can derive the SINR cdf averaged over n and average data rate in the same way as the single-user-single-resource-block case under the perfect CSI assumption.

The performance degradation due to the imperfect CSI condition is determined by two factors: the probabilities of selecting users other than the user with the highest fading gain and the gap between the SINRs of the user actually selected and the user with highest fading gain. Our results mainly contribute to the analysis of the latter factor.

Note that even if the observation model of fading gains is simple, the dependence of $h_{(1,n)}, h_{(2,n)}, \dots, h_{(n,n)}$ makes it difficult to write $p_{(i,n)}^{\text{sche}}$ ($i = 1, 2, \dots, n$) as a simple expression. However, the Monte Carlo estimation of these probabilities costs much less than the total evaluation of SINR distribution. The actual evaluation is found in Section V-B.

V. NUMERICAL EVALUATIONS

A. Validation Through Simulations

First, we validate the analytical results of SINR cdf through simulations. Unless otherwise specified, we set the path loss exponent $\eta = 4$, noise power $\sigma^2 = -90$ dBm, maximum transmit power $P_M = 23$ dBm, BS density $\lambda_{\text{BS}} = 2$ BSs/km², power-related constant $\rho_o = -70$ dBm, power control factor $\epsilon = 1$, and average number of users per BS $\lambda_{\text{UE}}/\lambda_{\text{BS}} = 4$. Each simulation is repeated 10,000 times, and the corresponding empirical cdf is shown.

Fig. 4 shows the SINR ccdfs for the cases of $\lambda_{\text{BS}} = 0.2, 2, 20$ BSs/km². In all cases, the figures also include three analytical results (19) for $i = 1, 2, 3$. Note that the achievable range R_d varies depending on ρ_o as $R_d = (P_M/\rho_o)^{1/\eta}$. We can see that for $i = 1, 2$, the analytical results averaged over $f_n^{(i)}(n)$ coincide with the simulation results when

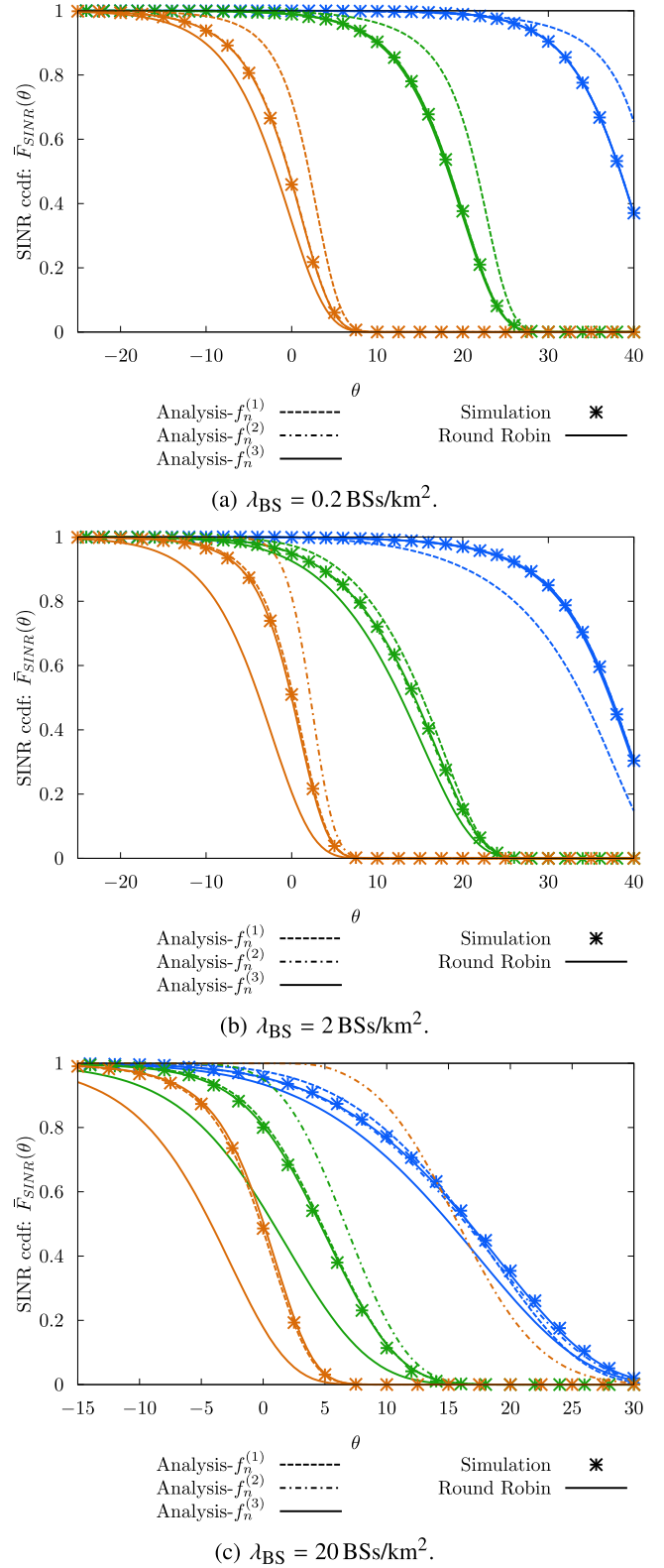


Fig. 4. SINR ccdfs $\bar{F}_{\text{SINR}}(\theta)$ obtained through a theoretical analysis and simulation (orange, green, and blue lines correspond to $\rho_o = -90, -70, -50$, respectively).

$g_i(\lambda_{\text{BS}}, R_d)$ is large. For example, $g_1 = 0.940$ for $\lambda_{\text{BS}} = 20$ BSs/km², $\rho_o = -70$ dBm and $g_2 = 0.894$ for $\lambda_{\text{BS}} = 0.2$ BSs/km², $\rho_o = -70$ dBm, which explains the good agreement between the simulation and analytical results averaged

TABLE I
PARAMETER SETTINGS IN THE NUMERICAL EVALUATION
(WITH DEFAULT VALUES INDICATED IN BOLD>)

Parameter	Value
Path loss exponent: η	4
Noise power: σ^2	0 mW, -90 dBm
Maximum transmit power: P_M	23 dBm
Power-related constant: ρ_o	-90, -70 , -50 dBm
BS density: λ_{BS}	0.2, 2 , 20 BSs/km ²
Average number of users per BS: $\lambda_{UE}/\lambda_{BS}$	4
Power control factor: ϵ	0, 0.25, 0.5, 0.75, 1

over $f_n^{(1)}(n)$ or $f_n^{(2)}(n)$. By contrast, neither of the two analytical results explains all simulation results simultaneously. We would like to emphasize that the analytical result using $f_n^{(3)}(n)$ accounts for the simulation results regardless of the BS density λ_{BS} and ρ_o .

Each figure also shows the multi-user diversity gain, which means that the SINR of the normalized SNR-based scheduling is superior to that of the round-robin scheduling, particularly within a low SINR region. Note that some of the results show a subtle improvement in the SINR, which derives from the fact that an insufficient number of candidate users exist to obtain multi-user diversity gain.

B. Validation Under Imperfect CSI Assumption

This section is devoted to the evaluation under the incomplete CSI assumption, which is discussed in Section IV-B, and we validate the analytical result (33) through a comparison with the Monte Carlo simulations. In this evaluation, we use $f_n^{(3)}(n)$ for the number distribution of candidate users, which shows a good agreement with simulation results for any λ_{BS} . To show the degradation of multi-user diversity clearly, we evaluate the SINR ccdf for the case of $\lambda_{BS} = 20$ BSs/km². This is the case in which the gap between normalized SNR-based scheduling and round-robin scheduling is clear, as shown in Fig. 4.

In this evaluation, we estimate $p_{(i,n)}^{\text{sche}}$ ($i = 1, 2, \dots, n$) under the assumption that the scheduler observes fading gains contaminated with additive i.i.d. Gaussian noise, which is used to evaluate (33). We assume that the observation model is a mapping from h_i to $\tilde{h}_i = |\sqrt{h_i} + z_i|^2$, where z_i is an i.i.d. complex Gaussian random variable [34] with zero mean and variance of 1/4.¹ The value of the variance is determined such that some, but not too many, errors occur with user selection (i.e., $p_{(1,n)}^{\text{sche}} \simeq 1/n$ and $p_{(n,n)}^{\text{sche}} \simeq 1$). Fig. 5 shows the estimated $p_{(i,n)}^{\text{sche}}$, $n = 2, 3, 4, 5$ for reference, which is obtained through 100,000-times simulations for each n .

Fig. 6 shows both the theoretical and simulation results under the imperfect CSI assumption, with the simulation results under the perfect CSI assumption given for reference.

¹The mapping is obtained in detail as follows. As discussed in [34], the noisy channel estimate of user i in the complex signal space is given as $\sqrt{h_i}e^{j\theta} + z_i$, where j is a imaginary unit, θ is a phase constant, and z_i is an i.i.d. circularly-symmetric complex Gaussian noise. Note that h_i is used to denote a channel power gain in this paper. Therefore, the estimated channel power gain is given by $\tilde{h}_i = |\sqrt{h_i}e^{j\theta} + z_i|^2 = |\sqrt{h_i} + z_i e^{-j\theta}|^2 = |\sqrt{h_i} + z_i'|^2$, where $z_i' = z_i e^{-j\theta}$. Considering the circular symmetry of z_i , z_i' can be seen as an i.i.d. circularly-symmetric complex Gaussian random variable.

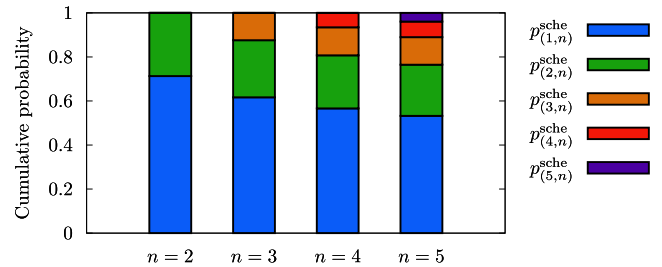


Fig. 5. Results of Monte Carlo estimation of $(p_{(1,n)}^{\text{sche}}, p_{(2,n)}^{\text{sche}}, \dots, p_{(n,n)}^{\text{sche}})$, $n = 2, 3, 4, 5$, each of which is the probability that the user with the i th largest fading gain $h_{(i,n)}$ is scheduled.

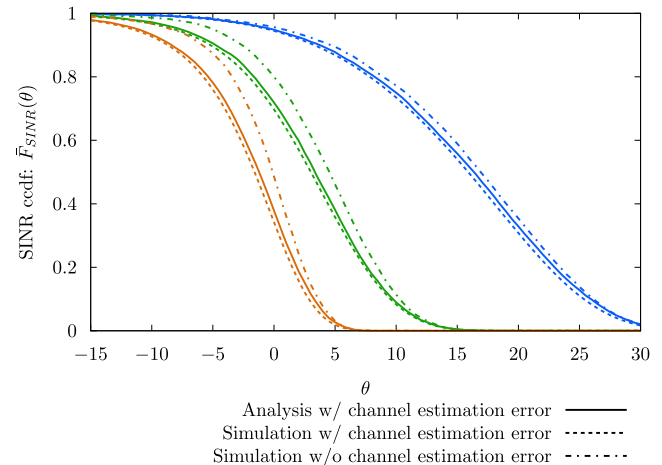


Fig. 6. SINR ccdfs $\bar{F}_{SINR}(\theta)$ obtained through a theoretical analysis and that of simulations under the imperfect CSI assumption for $\lambda_{BS} = 20$ BSs/km² (orange, green, and blue lines correspond to $\rho_o = -90, -70, -50$, respectively).

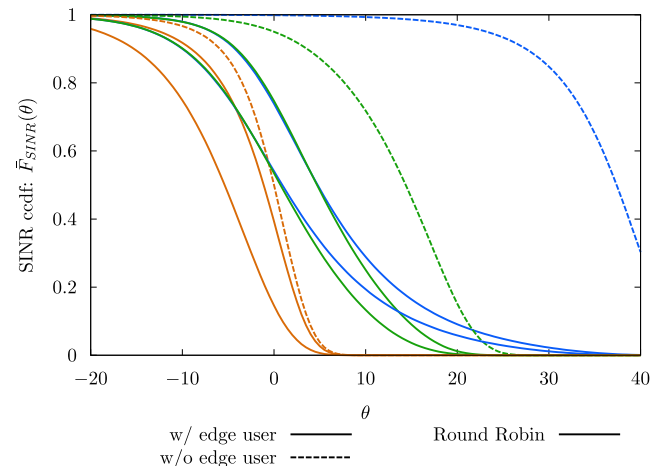


Fig. 7. SINR ccdfs when outage users are allowed and are not allowed to transmit (orange, green, and blue lines correspond to $\rho_o = -90, -70, -50$, respectively).

The results under the imperfect CSI assumption is, as a matter of course, inferior to the results under the perfect CSI assumption, and we can see that the theoretical results demonstrate the SINR degradation caused by the imperfect CSI.

C. SINR Distribution for General Power Control Policy

Fig. 7 shows the SINR ccdfs with edge users, who transmit at the maximum transmit power. We can also find that the

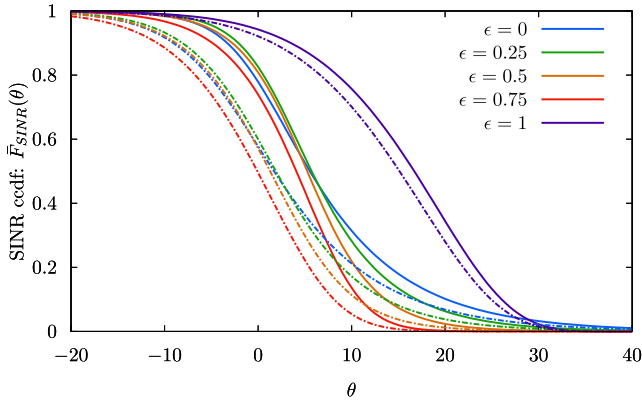


Fig. 8. SINR ccdfs when changing the value of ϵ (i.e., channel inversion is partially achieved) with $\sigma^2 = 0$ mW. The dashed lines represent the corresponding curves under round-robin scheduling.

SINR of the normalized SNR-based scheduling is superior to that of the round-robin scheduling. In addition, we can see that the SINR with edge users is inferior to that without edge users, particularly when ρ_o is large (i.e., the fraction of edge users $g_1(\lambda_{BS}, R_d)$ is large).

Fig. 8 shows the SINR ccdfs as a function of the fractional power control factor ϵ . We can also find the multi-user diversity gain. Note that the value of the fraction of edge users $g_1(\lambda_{BS}, R_d)$ varies depending on the value of ϵ (i.e., $g_1(\lambda_{BS}, R_d) = 0, 0, 0, 4.7 \times 10^{-5}, 0.76$ for $\epsilon = 0, 0.25, 0.5, 0.75, 1$, respectively). We can see that the SINR cdf for $\epsilon = 1$ exhibits a special behavior as compared to the other ccdfs. This result will contribute to determining the appropriate ϵ based on the system requirements.

D. Scheduling Gain Analysis

In this section, we evaluate the theoretical scheduling gain $G(\lambda_{BS}, \lambda_{UE})$ to investigate concrete numerical values and to review an example of how the gain changes with parameters.

Fig. 9 shows the scheduling gains $G(\lambda_{BS}, \lambda_{UE})$ as the number of users per BS varies. Each figure shows that the scheduling gain grows along with the number of users per BS, which explains the multi-user diversity. We can see that as the value of ρ_o , which represents the required signal power for $\epsilon = 1$, decreases, the scheduling gain increases. Note that the function $\log x$ increases more sharply for a smaller argument. Therefore, a user with a low SNR tends to obtain more scheduling gain than a user with a high SNR.

Fig. 9(b) shows the scheduling gains when edge users are allowed to transmit at the maximum transmit power. Compared to Fig. 9(a) (i.e., a case in which edge users are not allowed to transmit), in this figure we can see that the scheduling gain increases for any ρ_o and λ_{BS} . This is because of the increase in the number of candidate users and in the number of users with low required signal powers. Note that when the edge users are not allowed to transmit, these users do not contribute to the scheduling gain because they are not considered to be scheduled and the derived data rate is the average data rate of the scheduled users.

Fig. 9(c) shows the scheduling gains for different values of ϵ . We can see that the scheduling gain varies depending

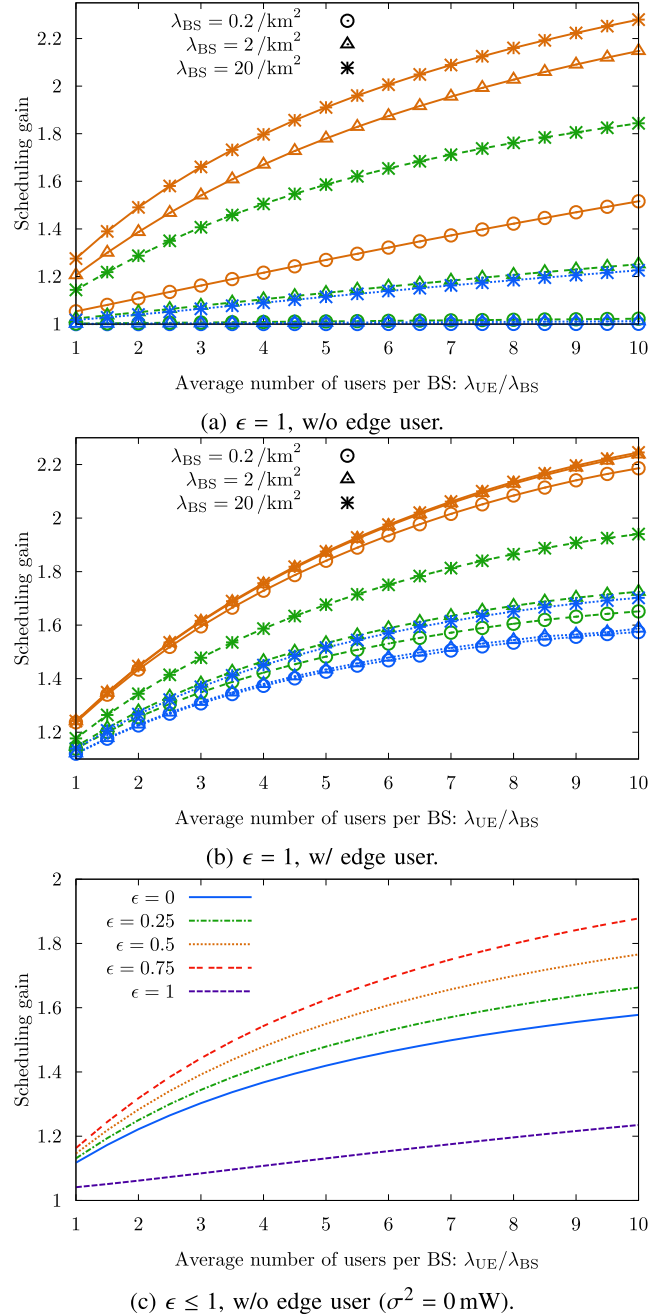


Fig. 9. Scheduling gain analyses (orange, green, and blue lines correspond to $\rho_o = -90, -70, -50$, respectively.)

on the value of ϵ . Therefore, we should consider the effect of the scheduling gain, in addition to the traditional consideration found in studies such as [7].

In all cases, we can also observe a performance gap between the round-robin scheduling and the normalized SNR-based scheduling. We can conclude that the analytical results derived from this study successfully capture the multi-user diversity.

VI. CONCLUSION

This study presented a new framework for analyzing the SINR distribution of a typical scheduled user in an uplink cellular network. In particular, the SINR distribution with a normalized SNR-based scheduler was obtained using stochastic geometry. One of the main observations was that the

multi-user diversity gain depends on the number of candidate users. Therefore, this study provided the averaged SINR distribution by considering the conditional SINR distribution given the number of candidate users and the number distribution of the candidate users in order. The number of candidate users in a typical cell was obtained in a general form by modeling the area of the existing range of candidate users with a beta distribution. The analytical SINR cdfs were in good agreement with the simulation results regardless of the transmit power control policy.

Numerical evaluations showed that the analytical results were in good agreement with the simulation results and highlighted the gap of the SINR cdf between round-robin scheduling and normalized SNR-based scheduling. We also observed that the resulting scheduling gain varies depending on the transmit power control policy and the number of accommodated users in each cell. In this sense, the given analytical framework provides a unified design method for estimating multi-user diversity for uplink cellular networks, enabling a performance evaluation that avoids underestimation that occurs when channel-adaptive user scheduling is not considered.

APPENDIX A

REST OF PROOF OF LEMMA 1

Considering that the scheduled users constitute a homogeneous PPP with intensity $(1 - f_n(0))\lambda_{\text{BS}}$, and that their transmit powers are independent random values, we obtain

$$\begin{aligned} \mathcal{L}_I(s) &= \mathbb{E}[e^{-sI}] = \mathbb{E}_{\Phi_{\text{su}}, \{g_u\}, \{p_u\}} \left[e^{-s \sum_{u \in \Phi_{\text{su}} \setminus \{u_o\}} p_u g_u \|u\|^{-\eta}} \right] \\ &= \mathbb{E}_{\Phi_{\text{su}}, \{g_u\}, \{p_u\}} \left[\prod_{u \in \Phi_{\text{su}}} e^{-s \mathbb{1}_{\{\|u\| > r\}} p_u g_u \|u\|^{-\eta}} \right] \\ &= \mathbb{E}_{\Phi_{\text{su}}} \left[\prod_{u \in \Phi_{\text{su}}} \mathbb{E}_{g,p} \left[e^{-s \mathbb{1}_{\{\|u\| > r\}} p g \|u\|^{-\eta}} \right] \right] \quad (34) \\ &\stackrel{(a)}{=} \exp \left(-c \int_0^\infty \mathbb{E}_p \left[1 - \mathbb{E}_g \left[e^{-s \mathbb{1}_{\{x > r\}} p g x^{-\eta}} \right] \right] x dx \right) \\ &= \exp \left(-c \cdot \mathbb{E}_p \left[\int_r^\infty \left(1 - \mathbb{E}_g \left[e^{-s p g x^{-\eta}} \right] \right) x dx \right] \right) \\ &= \exp \left(-c \cdot \mathbb{E}_p \left[\int_r^\infty \left(1 - \frac{1}{1 + s p x^{-\eta}} \right) x dx \right] \right) \\ &= \exp \left(\frac{c s r^{2-\eta}}{\eta-2} \mathbb{E}_p \left[p {}_2F_1 \left(1, 1 - \frac{2}{\eta}; 2 - \frac{2}{\eta}; -s p r^{-\eta} \right) \right] \right), \quad (35) \end{aligned}$$

where $c := 2\pi(1 - f_n(0))\lambda_{\text{BS}}$, and (a) follows from the probability generation functional of PPP [2]. Substituting $s = k\theta/r^{\eta(\epsilon-1)}\rho_o$ into $\mathcal{L}_I(s)$, we obtain the result of the lemma.

APPENDIX B

PROOF OF COROLLARY 1

Substituting $\epsilon = 1$ into (9) yields

$$\mathbb{P}(\text{SINR} > \theta | n) = \sum_{k=1}^n \binom{n}{k} (-1)^{k+1} \mathbb{E}_r \left[e^{-\frac{k\theta\sigma^2}{\rho_o}} \mathcal{L}_I \left(\frac{k\theta}{\rho_o} \right) \right]. \quad (36)$$

Note that $\mathcal{L}_I(s)$ depends on r , which is found in (34). Notice that we can remove u_o from the summation by $\mathbb{1}_{\{p_u \|u\|^{-\eta} < \rho_o\}}$ or equivalently $\mathbb{1}_{\{\|u\| > (p_u/\rho_o)^{1/\eta}\}}$ instead of $\mathbb{1}_{\{\|u\| > r\}}$. Then, we can obtain the Laplace transform of I , which is independent of r :

$$\begin{aligned} \mathcal{L}_I(s) &= \mathbb{E}_{\Phi_{\text{su}}, \{g_u\}, \{p_u\}} \left[\prod_{u \in \Phi_{\text{su}}} e^{-s \mathbb{1}_{\{\|u\| > (p_u/\rho_o)^{1/\eta}\}} p_u g_u \|u\|^{-\eta}} \right] \\ &= \mathbb{E}_{\Phi_{\text{su}}} \left[\prod_{u \in \Phi_{\text{su}}} \mathbb{E}_{g,p} \left[e^{-s \mathbb{1}_{\{\|u\| > (p/\rho_o)^{1/\eta}\}} p g \|u\|^{-\eta}} \right] \right] \quad (37) \\ &= \exp \left(-c \cdot \mathbb{E}_p \left[\int_{(p/\rho_o)^{1/\eta}}^\infty \left(1 - \frac{1}{1 + s p x^{-\eta}} \right) x dx \right] \right) \\ &\stackrel{(a)}{=} \exp \left(-c s^{2/\eta} \mathbb{E}_p [p^{2/\eta}] \int_{(s\rho_o)^{-1/\eta}}^\infty \frac{y}{y^\eta + 1} dy \right). \quad (38) \end{aligned}$$

Here (a) is followed by $y = x/(sp)^{1/\eta}$. Such an approach can be found in [8]. In addition, $\mathbb{E}_p [p^{2/\eta}]$ was obtained in [8] as:

$$\mathbb{E}_p [p^{2/\eta}] = \frac{\rho_o^{2/\eta} \gamma(2, \pi \lambda_{\text{BS}} R_d^2)}{\pi \lambda_{\text{BS}} (1 - e^{-\pi \lambda_{\text{BS}} R_d^2})}, \quad (39)$$

which is averaged over the distribution of the transmit power (6) with $\epsilon = 1$. Substituting $s = k\theta/\rho_o$ into (38) yields

$$\begin{aligned} \mathcal{L}_I \left(\frac{k\theta}{\rho_o} \right) &= \exp \left(- \frac{2(k\theta)^{2/\eta} \gamma(2, \pi \lambda_{\text{BS}} R_d^2) \int_{(k\theta)^{-1/\eta}}^\infty \frac{y}{y^\eta + 1} dy}{(1 - e^{-\pi \lambda_{\text{BS}} R_d^2}) / (1 - f_n(0))} \right) \\ &= \exp \left(- \frac{2k\theta \gamma(2, \pi \lambda_{\text{BS}} R_d^2) {}_2F_1 \left(1, 1 - \frac{2}{\eta}; 2 - \frac{2}{\eta}; -k\theta \right)}{(\eta - 2) (1 - e^{-\pi \lambda_{\text{BS}} R_d^2}) / (1 - f_n(0))} \right). \quad (40) \end{aligned}$$

Finally, substituting (40) into (36) and averaging with respect to r yield (10).

APPENDIX C

PROOF OF COROLLARY 4

We have

$$\begin{aligned} \tau_s(\lambda_{\text{BS}}, \lambda_{\text{UE}}) &= \int_0^\infty \mathbb{P}(\ln(1 + \text{SINR}) > t) dt \\ &= \int_0^\infty \mathbb{P}(\text{SINR} > e^t - 1) dt \\ &= \int_0^\infty \bar{F}_{\text{SINR}}(e^t - 1) dt \\ &= \int_0^\infty \frac{\bar{F}_{\text{SINR}}(x)}{x + 1} dx \\ &= \mathbb{E}_{n>0} \left[\sum_{k=1}^n \binom{n}{k} (-1)^{k+1} \mathbb{E}_r \right. \\ &\quad \left. \times \left[\int_0^\infty \frac{e^{-\frac{kx\sigma^2}{\rho_o r^{\eta(\epsilon-1)}}}}{x + 1} \mathcal{L}_I \left(\frac{kx}{\rho_o r^{\eta(\epsilon-1)}} \right) dx \right] \right]. \quad (41) \end{aligned}$$

(36) The simplification is given by considering (11).

REFERENCES

- [1] F. Baccelli and B. Błaszczyszyn, *Stochastic Geometry for Wireless Networks: Applications*, vol. 2. Boston, MA, USA: Now, 2009.
- [2] M. Haenggi, *Stochastic Geometry for Wireless Networks*. Cambridge, U.K.: Cambridge Univ. Press, 2012.
- [3] H. Elsawy, A. Sultan-Salem, M.-S. Alouini, and M. Z. Win, "Modeling and analysis of cellular networks using stochastic geometry: A tutorial," *IEEE Commun. Surv. Tuts.*, vol. 19, no. 1, pp. 167–203, 1st Quart., 2017.
- [4] H. Elsawy, E. Hossain, and M. Haenggi, "Stochastic geometry for modeling, analysis, and design of multi-tier and cognitive cellular wireless networks: A survey," *IEEE Commun. Surv. Tuts.*, vol. 15, no. 3, pp. 996–1019, 3rd Quart., 2013.
- [5] J. G. Andrews, F. Baccelli, and R. K. Ganti, "A tractable approach to coverage and rate in cellular networks," *IEEE Trans. Commun.*, vol. 59, no. 11, pp. 3122–3134, Nov. 2011.
- [6] "Digital design for 5G: A disruptive use case-driven approach," Nokia Netw., Espoo, Finland, White Paper, 2019.
- [7] T. D. Novlan, H. S. Dhillon, and J. G. Andrews, "Analytical modeling of uplink cellular networks," *IEEE Trans. Wireless Commun.*, vol. 12, no. 6, pp. 2669–2679, Jun. 2013.
- [8] H. Elsawy and E. Hossain, "On stochastic geometry modeling of cellular uplink transmission with truncated channel inversion power control," *IEEE Trans. Wireless Commun.*, vol. 13, no. 8, pp. 4454–4469, Aug. 2014.
- [9] H. Y. Lee, Y. J. Sang, and K. S. Kim, "On the uplink SIR distributions in heterogeneous cellular networks," *IEEE Commun. Lett.*, vol. 18, no. 12, pp. 2145–2148, Dec. 2014.
- [10] S. Singh, X. Zhang, and J. G. Andrews, "Joint rate and SINR coverage analysis for decoupled uplink–downlink biased cell associations in HetNets," *IEEE Trans. Wireless Commun.*, vol. 14, no. 10, pp. 5360–5373, Oct. 2015.
- [11] K. Smiljković, P. Popovski, and L. Gavrilovska, "Analysis of the decoupled access for downlink and uplink in wireless heterogeneous networks," *IEEE Wireless Commun. Lett.*, vol. 4, no. 2, pp. 173–176, Apr. 2015.
- [12] M. Di Renzo and P. Guan, "Stochastic geometry modeling and system-level analysis of uplink heterogeneous cellular networks with multi-antenna base stations," *IEEE Trans. Commun.*, vol. 64, no. 6, pp. 2453–2476, Jun. 2016.
- [13] E. Dahlman, S. Parkvall, and J. Skold, *4G: LTE/LTE-Advanced for Mobile Broadband*. New York, NY, USA: Academic, 2013.
- [14] P. Viswanath, D. Tse, and R. Laroia, "Opportunistic beamforming using dumb antennas," *IEEE Trans. Inf. Theory*, vol. 48, no. 6, pp. 1277–1294, Jun. 2002.
- [15] T. Ohto, K. Yamamoto, S.-L. Kim, T. Nishio, and M. Morikura, "Stochastic geometry analysis of normalized SNR-based scheduling in downlink cellular networks," *IEEE Wireless Commun. Lett.*, vol. 6, no. 4, pp. 438–441, Aug. 2017.
- [16] K. Yamamoto, "SIR distribution and scheduling gain of normalized SNR scheduling in Poisson networks," in *Proc. SpaSWin Conjoint WiOpt*, Shanghai, China, May 2018, pp. 1–6.
- [17] L. Yang and M.-S. Alouini, "Performance analysis of multiuser selection diversity," *IEEE Trans. Veh. Technol.*, vol. 55, no. 6, pp. 1848–1861, Nov. 2006.
- [18] H. A. David and H. N. Nagaraja, *Order Statistic*, 3rd ed. Hoboken, NJ, USA: Wiley, 2004.
- [19] S. Borst, "User-level performance of channel-aware scheduling algorithms in wireless data networks," *IEEE/ACM Trans. Netw.*, vol. 13, no. 3, pp. 636–647, Jun. 2005.
- [20] J.-G. Choi and S. Bahk, "Cell-throughput analysis of the proportional fair scheduler in the single-cell environment," *IEEE Trans. Veh. Technol.*, vol. 56, no. 2, pp. 766–778, Mar. 2007.
- [21] B. Błaszczyszyn and M. K. Karray, "Fading effect on the dynamic performance evaluation of OFDMA cellular networks," in *Proc. Int. Conf. Commun. Netw. (ComNet)*, Hammamet, Tunisia, Nov. 2009, pp. 1–8.
- [22] J. García-Morales, G. Femenias, and F. Riera-Palou, "Channel-aware scheduling in FFR-aided OFDMA-based heterogeneous cellular networks," in *Proc. IEEE CIT/UC/COM/DASC/PICOM*, Liverpool, U.K., Oct. 2015, pp. 44–51.
- [23] Y. Wang, M. Haenggi, and Z. Tan, "The meta distribution of the sir for cellular networks with power control," *IEEE Trans. Commun.*, vol. 66, no. 4, pp. 1745–1757, Apr. 2018.
- [24] S. Kamiya, K. Yamamoto, S.-L. Kim, T. Nishio, and M. Morikura, "Asymptotic analysis of normalized SNR-based scheduling in uplink cellular networks with truncated channel inversion power control," in *Proc. IEEE ICC*, Kansas City, MO, USA, May 2018, pp. 1–6.
- [25] S. M. Yu and S.-L. Kim, "Downlink capacity and base station density in cellular networks," in *Proc. Int. Symp. Modeling Optim. Mobile, Ad Hoc, Wireless Netw. (WiOpt)*, Tsukuba, Japan, May 2013, pp. 119–124.
- [26] S. Akoum and R. W. Heath, "Interference coordination: Random clustering and adaptive limited feedback," *IEEE Trans. Signal Process.*, vol. 61, no. 7, pp. 1822–1834, Apr. 2013.
- [27] C. U. Castellanos *et al.*, "Performance of uplink fractional power control in UTRAN LTE," in *Proc. IEEE VTC Spring*, Singapore, May 2008, pp. 2517–2521.
- [28] A. AlAmmouri, H. Elsawy, and M.-S. Alouini, "Load-aware modeling for uplink cellular networks in a multi-channel environment," in *Proc. IEEE PIMRC*, Washington, DC, USA, Sep. 2014, pp. 1591–1596.
- [29] A. Goldsmith, *Wireless Communications*. Cambridge, U.K.: Cambridge Univ. Press, 2005.
- [30] M. Haenggi, "The meta distribution of the SIR in Poisson bipolar and cellular networks," *IEEE Trans. Wireless Commun.*, vol. 15, no. 4, pp. 2577–2589, Apr. 2016.
- [31] J.-S. Ferenc and Z. Nédá, "On the size distribution of poisson Voronoi cells," *Phys. A, Stat. Mech. Appl.*, vol. 385, no. 2, pp. 518–526, Nov. 2007.
- [32] F. Berggren and R. Jantti, "Asymptotically fair transmission scheduling over fading channels," *IEEE Trans. Wireless Commun.*, vol. 3, no. 1, pp. 326–336, Jan. 2004.
- [33] L. Dai, B. Wang, Y. Yuan, S. Han, C.-L. I, and Z. Wang, "Non-orthogonal multiple access for 5G: Solutions, challenges, opportunities, and future research trends," *IEEE Commun. Mag.*, vol. 53, no. 9, pp. 74–81, Sep. 2015.
- [34] C. Wang, E. Au, R. Murch, W. Mow, R. Cheng, and V. Lau, "On the performance of the MIMO zero-forcing receiver in the presence of channel estimation error," *IEEE Trans. Wireless Commun.*, vol. 6, no. 3, pp. 805–810, Mar. 2007.



Shotaro Kamiya received the B.E. degree in electrical and electronic engineering from Kyoto University in 2015 and the M.E. degree from the Graduate School of Informatics, Kyoto University, in 2017, where he is currently pursuing the Ph.D. degree with the Graduate School of Informatics. From 2017 to 2019, he was a Research Fellow (DC1) of the Japan Society for the Promotion of Science (JSPS). He is a member of the IEICE. He received the TELECOM System Technology Award for Students, the Outstanding Paper Award for Young C&C Researchers, and the IEEE Kansai Section Student Award, in 2017, 2019, and 2019, respectively.



Koji Yamamoto (Member, IEEE) received the B.E. degree in electrical and electronic engineering from Kyoto University in 2002, and the master's and Ph.D. degrees in informatics from Kyoto University, in 2004 and 2005, respectively. From 2004 to 2005, he was a Research Fellow of the Japan Society for the Promotion of Science (JSPS). Since 2005, he has been with the Graduate School of Informatics, Kyoto University, where he is currently an Associate Professor. From 2008 to 2009, he was a Visiting Researcher at Wireless@KTH, Royal Institute of Technology (KTH), Sweden. He was a Tutorial Lecturer at ICC 2019. His research interests include radio resource management, game theory, and machine learning. He is a Senior Member of the IEICE and the Operations Research Society of Japan. He received the PIMRC 2004 Best Student Paper Award in 2004 and the Ericsson Young Scientist Award in 2006. He also received the Young Researcher's Award, the Paper Award, the SUEMATSU-Yasuharu Award from the IEICE of Japan in 2008, 2011, and 2016, respectively, and the IEEE Kansai Section GOLD Award in 2012. He serves as the Track Co-Chair for APCC 2017, CCNC 2018, APCC 2018, and CCNC 2019, and the Vice Co-Chair of the IEEE ComSoc APB CCC. He serves as an Editor for the IEEE WIRELESS COMMUNICATIONS LETTERS and the *Journal of Communications and Information Networks*.



Seong-Lyun Kim was an Assistant Professor of radio communication systems at the Department of Signals, Sensors and Systems, Royal Institute of Technology (KTH), Stockholm, Sweden. He was also a Visiting Professor at the Control Engineering Group, Helsinki University of Technology (now Aalto), Finland, the KTH Center for Wireless Systems, and the Graduate School of Informatics, Kyoto University, Japan. He is currently a Professor with the School of Electrical and Electronic Engineering, Yonsei University, Seoul, South Korea, heading the

Robotic and Mobile Networks Laboratory (RAMO). His research interests include radio resource management, information theory in wireless networks, collective intelligence, and robotic networks. He has served as a technical committee member or a chair for various conferences, and an editorial board member for the *IEEE TRANSACTIONS ON VEHICULAR TECHNOLOGY*, the *IEEE COMMUNICATIONS LETTERS*, *Elsevier Control Engineering Practice*, *Elsevier ICT Express*, and the *Journal of Communications and Network*. He has served as the leading Guest Editor for the *IEEE WIRELESS COMMUNICATIONS* and the *IEEE NETWORK FOR WIRELESS COMMUNICATIONS IN NETWORKED ROBOTICS*, and the *IEEE JOURNAL ON SELECTED AREAS IN COMMUNICATIONS*.



Takayuki Nishio (Member, IEEE) received the B.E. degree in electrical and electronic engineering and the master's and Ph.D. degrees in informatics from Kyoto University in 2010, 2012, and 2013, respectively. From 2016 to 2017, he was a Visiting Researcher at the Wireless Information Network Laboratory (WINLAB), Rutgers University, New Brunswick, NJ, USA. He is currently an Assistant Professor in communications and computer engineering with the Graduate School of Informatics, Kyoto University. His current research interests

include machine learning-based network control, machine learning in wireless networks, and heterogeneous resource management.



Masahiro Morikura received the B.E., M.E., and Ph.D. degrees in electronics engineering from Kyoto University, Kyoto, Japan, in 1979, 1981, and 1991, respectively. He joined NTT, in 1981, where he was engaged in the research and development of TDMA equipment for satellite communications. From 1988 to 1989, he was with the Communications Research Centre, Canada, as a Guest Scientist. From 1997 to 2002, he was active in the standardization of the IEEE 802.11a-based wireless LAN. He is currently a Professor with the Graduate

School of Informatics, Kyoto University. His current research interests include WLANs and M2M wireless systems. He received the Paper Award and the Achievement Award from IEICE, in 2000 and 2006, respectively. He also received the Education, Culture, Sports, Science and Technology Minister Award in 2007 and Maejima Award, in 2008, and the Medal of Honor with Purple Ribbon from Japan's Cabinet Office, in 2015.